PRELIMINARY DESIGN OF A MEMS STEAM TURBINE POWER PLANT-ON-A-CHIP

Luc G. Fréchette*, Changgu Lee, Selin Arslan, and Yuan-Chun Liu
Columbia University
Department of Mechanical Engineering

ABSTRACT

This paper presents the system-level and component design of a micro steam turbine power plant-on-a-chip which implements the Rankine cycle for micro power generation. The microfabricated device consists of a steam turbine that drives an integrated micropump and generator. Two-phase flow heat exchangers are also integrated on-chip with the rotating components to form a complete micro heat engine unit, converting heat to electricity. Expected power levels range from 1-12 W per chip with energy conversion efficiency in the range of 1-11%. This suggests power density of up to 12 kW/kg for this technology, which is an order of magnitude greater than competing technologies, such as thermoelectrics.

Keywords: MEMS, micro power generation, microturbine, micropump.

INTRODUCTION

The advent of microelectromechanical systems (MEMS) technology has opened the door to the creation of power systems at unprecedented small scales. Using silicon microfabrication processes, it has been suggested that common power generation systems could be miniaturized yielding high-power density, low-cost, batch manufactured power sources, or *Power MEMS* [1]. Since the mid-1990's, development efforts have been initiated to create MEMS-based heat engines, such as gas turbine engines ([2]-[4]), internal combustion engines (rotary Wankel [5] or piston [6]), and thermal-expansion-actuated piezoelectric power generators [7]. These microengines convert thermal energy (from combustion of a fuel or another heat source), sequentially into fluid, mechanical, then electrical energy.

The concept developed herein consists of a microfabricated steam turbine power plant-on-a-chip, delivering electricity by scavenging waste heat or through combustion of a fuel. The fabrication approach is based on lithography, deep reactive ion etching, and aligned bonding of silicon and glass wafers. This micro heat engine implements a closed Rankine power cycle using a high speed microturbine with an integrated pump and generator, as well as on-chip heat exchangers. Each power plant chip is expected to generate in the range of 1-10 Watts of electrical power and is nominally 3 mm thick by 1 cm^2 (planar form). A heat supply, heat sink, and power electronics are also required in order to form a complete power generation system.

A single micro Rankine device coupled with a fuel burner could be used as a compact power generator for portable electronics, distributed sensors, and other small scale applications. These micro heat engines could also be useful to generate power from solar radiation or scavenge energy from waste heat, acting for example as a bottoming cycle for other heat engines by covering the engine and exhaust with an array of such chips; the output power then scales proportionally with covered area. The core components would also provide a basis for micro-refrigeration cycles to cool electronics, sensors, or people, as well as micro hydraulic sources for small robots and vehicles. This initial development effort focused on two applications with significantly different ambient temperatures: 1) *Ground power generation*: device cooled with room temperature air (T_{amb}=25˚C) and forced convection is required (cooling fan); 2) *Aircraft in-flight power generation*, device cooled with ambient air (T_{amb}= -50˚C) and forced cooling is available from motion of the aircraft.

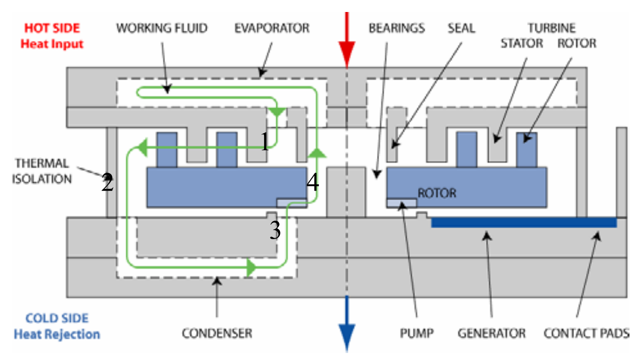

Figure 1 - Cross-section schematic of micro steam-turbine power plant-on-a-chip. Constructed from 5 silicon wafers that are deep reactive ion etched and bonded to integrate the components on a single chip.

SYSTEM-LEVEL DESIGN

Device Configuration

The simplified device configuration is shown in Figure 1. It consists of a multi-wafer stack that encloses all the components, including a disk-shaped rotor, microchannels, and electromechanical components. The rotor disk has a planar multistage turbine on one side and a micro-generator on the opposite side. A spiral groove viscous pump is etched at the inner radius of the disk, inboard of the generator, and delivers pressurized liquid through a center hole in the rotor disk (state 4). The pressurized working fluid then flows through a microchannel heat exchanger

* Corresponding author – 500 W. 120th St, MC4703, New York, NY 10025 USA, phone: (212) 854-2962; e-mail: lucf@alum.mit.edu

covering the hot side of the chip, to completely evaporate and be superheated (state 1). The vapor returns to the center to flow radially outwards along the top side of the rotor disk, through concentric turbine stages, each consisting of a stationary row of blades (attached to the top plate) interdigitated with a rotating blade row that extends from the disk. Vapor flow exiting the turbine (state 2) proceeds to the second microchannel heat exchanger located on the cold side of the chip to condense before returning to the pump (state 3). Seals are required on both sides of the disk to constrain the liquid within the pump and central area. Heat is supplied to the cycle from one outer surface of the chip ("hot side") and removed from the opposite surface ("cold side").

Fluid film bearings support the rotor in the radial and axial directions. A hydrostatic journal bearing is located at the outer diameter of the disk, lubricated by the pressurized working fluid in vapor state. Axial support is provided by a thrust bearing formed in the generator gap. The overall dimensions of the device are less than 3 mm thick x 1 cm^2.

The fabrication approach is based on silicon microfabrication technology. First, the electrical components are fabricated on silicon wafers using thin and thick film processing and lithography. Shallow features, such as tip clearance, seal gaps, and grooves for the viscous pumps, are then lithographically defined and etched. Deep structures, such as turbine blades and flow channels, are then formed into the bulk of the silicon wafers by deep reactive ion etching (DRIE) of lithographically-defined features on both sides of the wafers. The final device is formed by bonding the silicon wafers, creating a laminated, monolithic static structure with integrated quasi-three dimensional flow paths. This approach has been initially developed at MIT for the fabrication of high performance micro-machinery, such as micro gas turbine engines and generators [2], and was demonstrated to be viable for high speed rotation [8], high temperatures [9] and high pressures [10].

Cycle Analysis

Fundamentally, thermodynamics are not a function of scale. Practically however, component efficiencies are typically lower than their large scale brethren and high heat fluxes are required in the heat exchangers. Thermodynamic cycle analysis was performed for both applications in order to evaluate the potential performance of a Rankine cycle. Water is used as the working fluid, and component efficiencies of 5% for the pump and 70% for the turbine are assumed. To allow sufficient external heat removal from the condenser, high condenser temperatures were required. Optimum condenser temperatures of 93.5˚C and 10˚C were found for the ground and in-flight applications respectively, in order to maximize the net output electrical power. Thermodynamic cycle studies suggest that the efficiency and specific power increase with turbine inlet temperature and pressure, but with limited returns and reduced specific power above 4 MPa due to the increasing power requirement from the pump [11]. Performance is barely affected by pump efficiency for turbine inlet pressures below 4 MPa.

COMPONENT DESIGN

Turbine

Meanline modeling of the turbomachinery suggests that a power level of 1W (40 kJ/kg) per stage was achievable with conservative designs for the baseline mass flow of 24 mg/s. In order to match the specific power levels defined in the cycle analysis, 10 to 30 stages are expected to be required. It is difficult however to match more than 5 stages on a single rotor, since they operate with different tip speeds and flow areas dictated by the change of radius. A single rotor is therefore expected to provide on the order of 5 W of mechanical power (200 kJ/kg). The microturbine design and operating conditions are summarized in Table 1. Rotor and stator isentropic efficiencies of 70% are assumed, based on CFD analysis of microturbomachinery [12]. Since the rotor diameter is significantly less than the chip size, multiple spools (rotors) per chip can be used to achieve a broad range of power levels. Preliminary design was also developed for a 28 W (1150 kJ/kg) multiple rotor configuration, which consists of five individual rotors with power levels ranging from 3.8 to 8.4W. It operates with an inlet pressure of 8 MPa and temperature of 780°C.

Table 1 – Single-rotor microturbine configuration and operating conditions.

Inlet/Exit Pressure	0.60 to 0.18 MPa
Inlet/Exit Temp.	400°C to 316°C
Inner/Outer Radius	360 to 760 microns
Blade chord	Range: 20 to 50 microns
Flow exit angle (rel.)	60°, 4th rotor: 55°, 5th rotor: 50°
Mass flow	24 mg/s
Rotational speed	4×10^5 rad/s (tip speed 305 m/s)
Total power	5W

Pump

Given the very small volumetric flow rate of the working fluid in liquid form (1500 times less than in vapor phase) and the non-stringent requirement on pump efficiency, a spiral groove viscous pump was chosen and designed for this application. It consists of a polar array of shallow radial grooves inclined at a constant spiral angle, α, that rotate parallel to a planar surface.

Table 2 - Optimized configurations of low pressure and high pressure viscous pumps.

ΔP	0.6MPa	8MPa
Rotational speed	4×10^5 rad/s	4×10^5 rad/s
Spiral angle	15°	15°
Groove depth, h_1	4.6 μm	3.1 μm
Clearance, h_2	0.6 μm	0.5 μm
Inner radius, r_1	214 μm	243 μm
Outer radius, r_2	275 μm	450 μm
Power req'd	0.35 W	4.60 W
Efficiency	4.3 %	4.2 %

The configuration is readily micromachined on the back side of the rotor and integrated with the other Rankine device components. The pressure rise, torque and power consumption as a function of geometry, rotational speed and flow rate can be determined based on published work on macroscale spiral groove viscous pumps [13]. Over a broad range of pressure ratios (from 0.6 MPa to 8 MPa), optimized configurations were found with a maximum efficiency of 4-5%. Two configurations are summarized in Table 2 for low pressure and high pressure operation.

Heat Exchangers

The evaporator and condenser consist each of two main parts: internal two-phase flow heat exchange surfaces in contact with the working fluid and external heat transfer surface in contact with the heat source or heat sink. External heat sink optimization presented elsewhere [14] suggests that it is possible to remove 50-100W of heat per cm^2 by forced air convection with less than 1 W of fan power. Heat transfer and pressure drop in two-phase flow microchannels was also investigated to determine the potential configurations for the internal components. Based on traditional relations, the pressure drop in both sections was found to be only <2 % of the pump pressure rise for optimized configurations, which is small from a system perspective. The total required channel length was found to be less than 1 mm, suggesting that there is sufficient space in the $1cm^2$ chip to evaporate and condense the working fluid. Microchannel two-phase flow is however an on-going area of research and further development is required to devise a configuration that provides stable, superheated steam for this application.

Bearings and seals

Two types of bearings are required for the proposed device: thrust bearings for axial support and journal bearings for in-plane support of the rotor. In both cases, a fraction of the core pressurized flow is used to lubricate the bearings.

Axial balance - In order to axially balance the rotor on fluid films, the bottom side of the disk is used as a thrust balance piston, by drawing a small fraction of high pressure steam from the turbine inlet. The flow extracted from the turbine flow gets into the bottom side through holes or slits on the disk, and comes out of the bearing past a flow restriction at the outer radius, as illustrated by the flow path in Figure 2. The back-side pressure provides an upward force that compensates for the large downward force from the turbine and generator. At the given condition below, the flow rate for the axial balance is >10% of the flow rate through the turbine when the smallest gap is 1 micron. This configuration also provides a stabilizing (i.e. restoring) force when the rotor is perturbed from equilibrium. Stiffness levels up to 600,000 N/m are achievable at design conditions.

Journal bearing - Micro journal bearing experience to date is limited to gas lubricated bearing at the outer radius of 4 mm diameter rotors with 0.3 mm axial length, which have been demonstrated at high rotational speeds (up to 300 m/s tip speed) [8]. In order to minimize the development risks for the Rankine device, a similar configuration is designed herein. It requires journal pressure differentials on the order of 5-30 kPa, which are significantly lower than pressures available in the system.

Seals - As illustrated in Figure 2, seals are needed on the backside of the rotor to separate the pressurized liquid from entering the backside of the rotor, otherwise, viscous drag in the generator gap would overwhelm other forces on the rotor and drastically impact performance and efficiency. Calculations suggest that the planar clearance with a gap of 1 micron or less would lead to negligible leakage flow rate. A similar seal is implemented on the front side of the rotor, between the pump exit and turbine inlet streams.

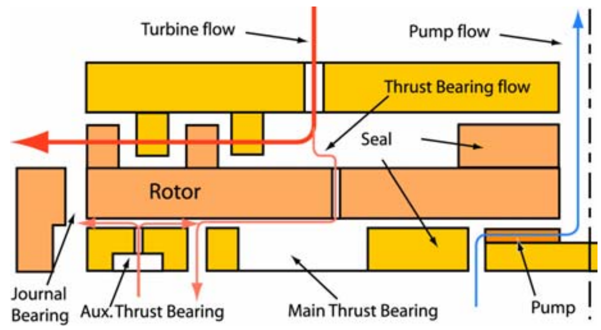

Figure 2 - Cross-section schematic showing the main and secondary flow paths. Axial balance is created by bleeding some of the turbine inlet steam under the disk, with the pressure controlled by the outer bearing.

Generator

The electromagnetic generator design will be directly based on the technology developed at MIT for Watt-scale, microfabricated motors and generators ([16]). Although specific design studies have not been carried out for the Rankine device, such electromechanical technology is expected to be appropriate since the operating conditions and fabrications constraints are similar, and even more conservative, that the gas turbine applications these are currently being developed for. Based on analysis and experiments to date, electromechanical energy conversion efficiency on the order of 50% is expected for such micro-motors and generators.

PREDICTED SYSTEM PERFORMANCE

The net output power will be equal to the cycle power minus viscous losses, such as bearing friction, seal drag, and disk windage (viscous drag other than in the bearings and seals), as well as ohmic losses in the generator and power electronics. Additional loss will also result from thermal conduction through the static structure. Thin SiO_2 walls are predicted to offer acceptable isolation while withstanding the internal pressure loads. Figure 3 presents the predicted performance for three different configurations: 1) the top bars are for a high superheated temperature (800°C) and high pressure (8 MPa) device operating in-flight (-50°C ambient); 2) the mid bars are also for in-flight application, but with a lower temperature (400°C) and pressure (0.6 MPa) device, and; 3) the lower bars are this same device, but for ground applications (25°C ambient). This last configuration requires active cooling with a fan that is driven by a fraction of the micro Rankine device output.

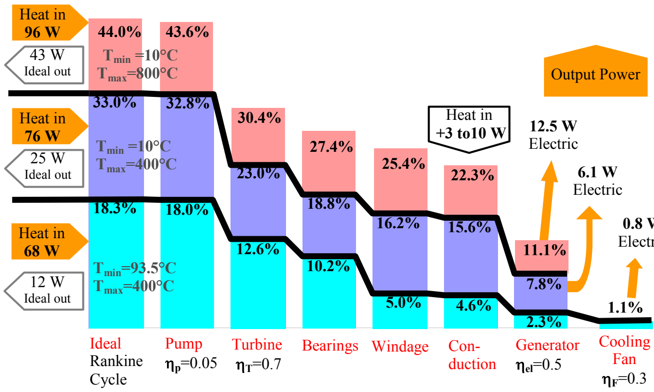

Figure 3 - Predicted performance of the Micro Steam Turbine Power Plant-on-a-chip for three configurations. Bars illustrate the reduction in power as the various sources of loss in the system are incrementally added, from left to right (water 24mg/s, P_{max}=0.6 MPa).

The output power is predicted to be on the order of 1-12 W for a total heat input of 70-110 W, which corresponds to an energy conversion efficiency of **1-11%** and a power density of **up to 12kW/kg**. Similar predictions suggests that the proposed technology has comparable efficiency with thermoelectric generators (6.5% for Rankine versus 4.5% for thermoelectrics) for similar operating temperatures (T_{max} = 230°C). The power density is however at least one order of magnitude higher for the micro Rankine device, on par with large scale gas turbine generators. Efficiency and power density can be even higher since the Rankine devices can operate at higher temperatures that allowed for thermoelectric materials. Cost benefits are also expected.

CONCLUSIONS

System-level and component design studies have been carried out for a miniature heat engine implementing the Rankine power cycle using MEMS-based, high performance micromachinery. These suggest that high power density microsystems (up to 12 kW/kg) for power generation appear possible, with efficiency levels on the order of 1-11%, depending on the application. The design space for micromachined multistage turbines and viscous pumps were explored to confirm that viable designs are possible for this application. Current research work is focusing on two key subsystems: 1) the rotating portion of the micro Rankine power plant-on-a-chip, which includes the multistage turbine, pump, bearings, and seals; and 2) the hot section, specifically the evaporator with a focus on robust configurations to provide a stable flow of superheated steam.

ACKNOWLEDGMENTS

Early discussions and contributions of Dr. Norbert Müller, Ying-Ting Yang, and Ajay Rishi are greatly appreciated. This work was supported by the NASA Glenn Research Center, Revolutionary Aeropropulsion and Power Concepts and Technology program (contract NAS3-02118), monitored by Dr. Glenn Beheim. The authors gratefully acknowledge this support.

REFERENCES

[1] Epstein A.H. and Senturia S.D., 1997, "Macro Power from Micro Machinery", Science, **276**, p.1211.

[2] Epstein, A.H., et al. 1997, "Micro-Heat Engines, Gas Turbines, and Rocket Engines - The MIT Microengine Project," AIAA Paper 97-1773, *28th AIAA Fluid Dynamics Conference*, Snowmass Village.

[3] Epstein A.H, Jacobson S.A., Protz J., Fréchette L.G., 2000, "Shirtbutton-Sized Gas Turbines: The Engineering Challenges of Micro High Speed Rotating Machinery," *Proc. 8th Int'l Symp. on Transport Phenomena and Dynamics of Rotating Machinery*, Honolulu, Hawaii.

[4] Isomura, K., et al., 2002, "Development of Microturbocharger and Microcombustor for a Three-Dimensional Gas Turbine at Microscale," *ASME IGTI 2002 TURBO EXPO*, Paper GT-2002-30580, Amsterdam, Netherlands, June 6.

[5] Fu, K., *et al.*, 2001, "Design and Fabrication of a Silicon-Based MEMS Rotary Engine," *Proc. ASME Int'l Mech. Eng. Congress and Expo.*, New York, Nov. 11-16.

[6] Toriyama, T., Hashimoto, K., Sugiyama, S., 2003, "Design of a Resonant Micro Reciprocating Engine for Power Generation," Proc. *Transducers'03*, Boston, MA, June.

[7] Richards, C.D., Bahr, D.F., Xu, C.-G., Richards, R.F., 2001, "The P3 Micro Power Generation System," *Proc. ASME Int'l Mech. Eng. Cong. & Expo.*, New York, Nov.

[8] Fréchette, L.G., Jacobson, S.A., Ehrich, F.F., Ghodssi, R., Khanna, R., Wong, C.W., Zhang, X., Schmidt, M.A., Epstein, A.H., 2000, "Demonstration of a Microfabricated High-Speed Turbine Supported on Gas Bearings," Tech. Digest, *Solid-State Sensor and Actuator Work.*, Hilton Head Is., SC, pp. 43-47.

[9] Mehra, A., *et al.*, 2000, "A Six-Wafer Combustion System for a Silicon Micro Gas Turbine Engine," *J. Microelectromechanical Syst.*, vol. 9, no. 4, pp. 517-527.

[10] London, A.P., Epstein, A. H., Kerrebrock, J. L., 2001, "High-Pressure Bipropellant Microrocket Engine," *AIAA J. Propulsion and Power*, vol. 17, no. 4, pp. 780-787.

[11] Meuller, N., Fréchette, L.G., "Performance Analysis of Brayton and Rankine Cycle Microsystems for Portable Power Generation". *Proc. 2002 ASME Int'l Mech. Eng. Congress and Expo.*, New Orleans, LA, Nov. 2002.

[12] Mehra, A., 1997, *Computational Investigation and Design of Low Reynolds Number Micro-Turbomachinery*. S.M. Thesis, MIT, Cambridge, MA.

[13] Hsing, F. C., 1974, "Analytical Solutions for Incompressible Spiral Groove Viscous Pumps," *ASME J. Lubrication Tech.*, vol. 96, no. 3, pp. 365-369.

[14] Meuller, N., Fréchette, L.G., 2002, "Optimization and Design Guidelines for High Flux Micro-Channel Heat Sinks for Liquid And Gaseous Single-Phase Flow," *Proc. 8th Intersociety Conf. on Thermal and Thermomech. Pheno. in Elec. Systems* (ITherm2002), San Diego, June.

[15] Zhang L., et al., 2001, "Study of boiling regimes and transient signal measurements in microchannels," *11th Int'l Conf. on Solid-State Sensors and Actuators*, Munich, Germany, June 10-14.

[16] Fréchette, L.G., Nagle, S.N., Ghodssi, R., Umans, S.D., Schmidt, M.A., Lang, J.H., "An Electrostatic Induction Micromotor Supported on Gas-Lubricated Bearings". *Proc. of 14th IEEE Int'l Micro Electro Mechanical Systems Conf.*, Interlaken Switzerland, Jan. 2001.